Gravity waves and vertical shear of zonal wind in the summer mesosphere-lower thermosphere

C. Jacobi and M. Ern

Summary

Gravity wave amplitudes and momentum fluxes derived from SABER temperature measurements are analysed together with Collm meteor radar zonal winds. The momentum flux (MF) divergence derived from the SABER temperatures shows a maximum that is found at greater altitudes during solar minimum than during solar maximum. Therefore, the zonal mean wind and wind shear profiles are shifted upwards then, leading to a modulation of the otherwise negative correlation between solar cycle and mesosphere/lower thermosphere winds.

Zusammenfassung

Amplituden von Schwerewellen und zugehörigen Impulsflüsse werden zusammen mit Windmessungen des Meteorradars Collm analysiert. Die Impulsflussdivergenz, abgeleitet aus SABER-Temperaturprofilen, hat ein Maximum welches im solaren Minimum nach oben verschoben ist. Dadurch werden auch die Vertikalprofile des Zonalwindes und der Windscherung nach oben verschoben, wodurch die ansonsten negative Sonnenfleckenzyklusabhängigkeit des zonalen Windes in der Mesosphäre/unteren Thermosphäre im solaren Minimum umgekehrt wird.

1 Introduction

The mesosphere-lower thermosphere (MLT) region is characterised by the interaction between gravity waves (GW) and the mean wind. During recent years, there has been considerable interest in the interannual and long-term variability of both mean winds and GW (e.g., Hoffmann et al., 2011; Jacobi et al., 2006, 2011, 2012) in order to detect long-term trends and a possible decadal (solar cycle) variation and to investigate coupling processes between mean winds and GW. While Hoffmann et al. (2011) essentially detected a positive long-term trend in MLT GW, Jacobi et al. (2006, 2011) found a strong solar cycle variation in summer GW proxies and mean winds. However, they also found a more complicated behaviour, so that during solar minimum the otherwise negative solar cycle effect on the mean wind is reversed.

Jacobi et al. (2011, 2012) had used LF winds measured at Collm (reference point is 52°N, 15°E near 90 km). The dataset and analysis procedure is described in Jacobi et al. (2012) for the prevailing wind and in Jacobi et al. (2006) for the GW proxies. Fig. 1 presents a height-time cross-section of GW proxies, being defined here as the squared difference between consecutive half-hourly mean LF winds provided that the reference height between these values does not change. Maximum GW variances are found in summer in the upper mesosphere. The known winter maximum is not visible, which may be due to the short periods (about 1 hr) the LF GW proxy is representative for.

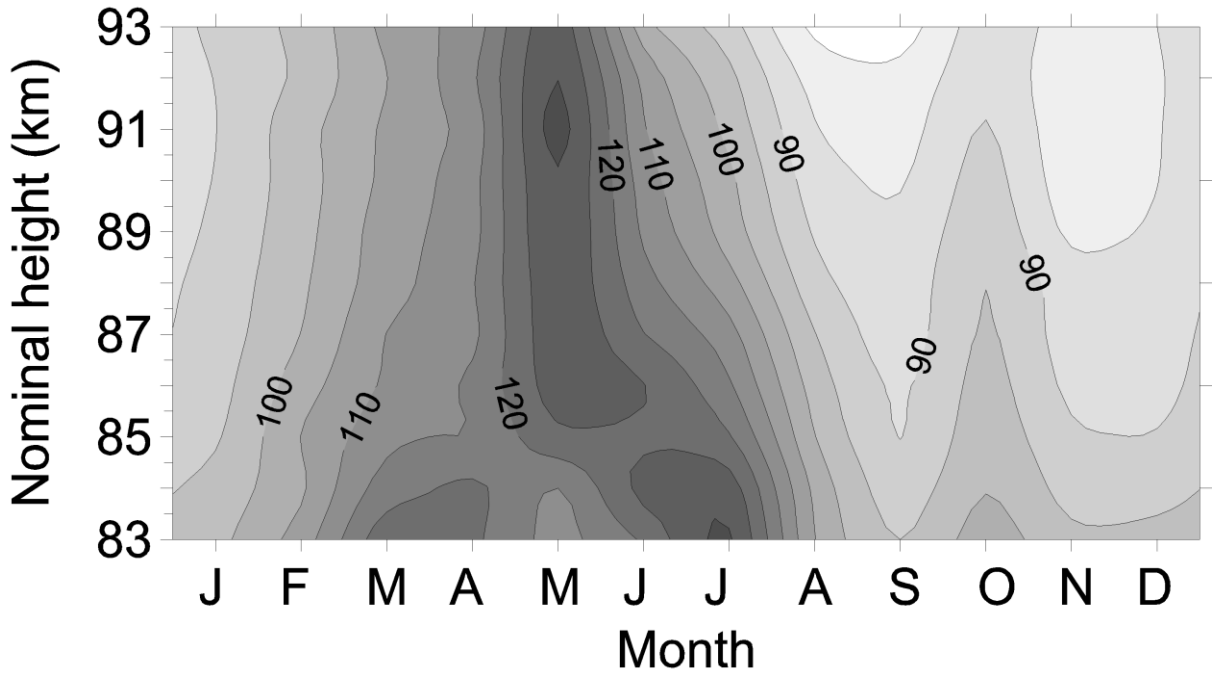

Figure 1: *1984-2007 mean GW variance proxy, calculated from the sum of differences between consecutive half-hourly mean zonal and meridional winds measured by the LF D1 method at Collm.*

Generally, the summer circulation is more stable than the winter one, and the interannual variability in summer is smaller than in winter, when planetary waves and stratospheric warmings may lead to significant effects in the MLT circulation on a monthly time scale. During summer, day-to-day variability may be caused by the quasi 2-day wave (e.g., Muller and Nelson, 1978) and a QBO effect on the MLT mean wind. However, while the former should cancel out if longer time intervals of one month or a full season are considered, the latter has been found to be insignificant during summer (Jacobi et al., 1996). Therefore, the analysis of the summer circulation is recommended if primarily GW effects on the MLT mean circulation are to be analysed.

Time series of summer (June–August, hereafter JJA) mean zonal prevailing winds at about 90 km and GW proxies (again, the sum of the squared zonal (U'^2) and meridional (V'^2) half-hourly mean wind deviations are used) at the same altitude are presented in Fig. 2, together with the F10.7 index, i.e. the solar radio flux at 2800 MHz given in sfu (1 sfu = 10^{-22} $Wm^{-2}Hz^{-1}$), as a solar activity proxy. Note that the height of 90 km for the winds and GW proxy has been calculated from the measured virtual LF reflection heights using an empirical formula that has been derived from winter vertical tidal phase profiles (Jacobi, 2011), so that there is a possible (and to a certain degree unknown) uncertainty of this value. Fig. 2 is very similar to another one presented by Jacobi et al. (2011, their Fig. 2), but there mean winds not decomposed into prevailing winds and tides have been shown and the sunspot number was presented instead of F10.7. However, the results are similar: there is a clear tendency for increasing GW activity during solar maximum, while the solar cycle effect of the prevailing wind is negative, i.e. there is a tendency for stronger eastward winds in the

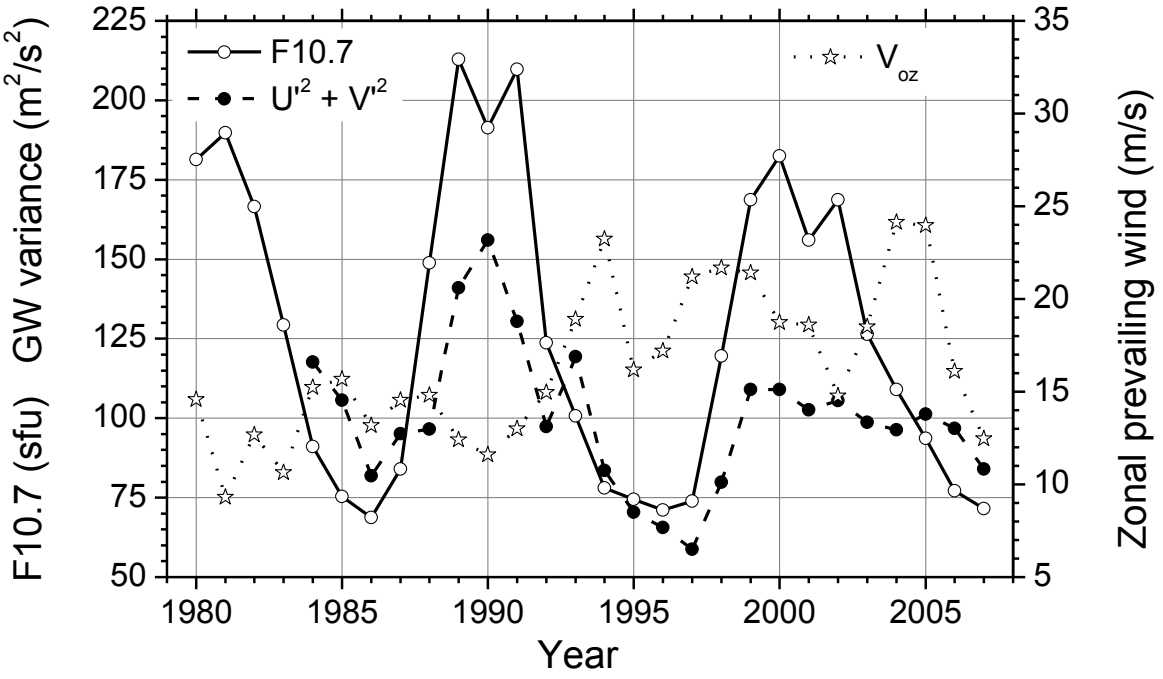

***Figure 2**: Time series of June-August mean zonal prevailing winds (open stars, Jacobi et al., 2012) and GW variance (solid circles) over Collm at approximately 90 km altitude, as derived from LF wind measurements. F10.7 is added as open circles.*

mesosphere during solar maximum. The latter can be explained by stronger mean circulation forcing of the middle atmosphere during solar maximum, leading to a stronger mesospheric wind jet then. This in turn may influence the filter characteristics of the wind jet, leading to larger GW amplitudes if the mean wind is stronger. The described tendencies can also be seen in the Juliusruh, Rügen, medium frequency radar wind data presented by Keuer et al. (2007) and also in Hoffman et al. (2011), but there the focus was laid on long-term trends.

There are, however, deviations from this simple picture, in particular an increase of GW amplitudes shortly after the solar maximum (in 1993 and, less pronounced, in 2005 in Fig. 2), and above all a reversal of the solar cycle–mean wind connection during solar minimum, so that in 1986, 1995/96 and after 2005 the prevailing winds decrease again. To get more insight into this behaviour, data from the extreme solar minimum 2008/2009 are required, as well as winds and GW analyses at different altitudes.

Since the LF measurements have been terminated after 2007, and since their vertical resolution is limited, in this study we apply the Collm VHF meteor radar winds since 2005 together with GW analyses from SABER temperature measurements, and analyse the interannual variability of zonal mean wind and GW amplitudes and momentum fluxes (MF).

2 Measurements and data analysis

Collm meteor radar zonal winds

The SKiYMET meteor radar located at Collm, Germany (51.3°N, 13°E) has been in operation nearly continuously since July 2004, and JJA means of the years 2005-2012 are used here. The radar measurements are described in Jacobi (2011, and references therein). The height interval is divided into six non-overlapping height gates, centred at about 82, 85, 88, 91, 94 and 97 km. Zonal prevailing winds are calculated applying least-squares fitting of mean winds and tidal variations on one month of half-hourly horizontal winds.

GW variances and momentum fluxes can also be derived from fitting 2-hourly mean of these data to the individual radial winds (Hocking, 2005; Placke et al., 2011). However, there is a considerable amount of uncertainty in these analyses, and the height resolution is limited, so that they are only briefly presented here to substantiate the results.

SABER GW analyses

GW amplitudes are calculated from SABER temperature profiles. Before, planetary waves have been removed from the profiles as described in Ern et al. (2011), while tides have been analysed as stationary planetary-scale structure for ascending and descending nodes. Subtracting these average local background temperatures T from the measurements we obtain altitude profiles of residual temperatures that are dominated by GWs. Squared temperature amplitudes $\hat{T}$ have been calculated from the residual temperatures in a 10 km sliding vertical window at 1 km step, and using the data within a window of 10° in latitude (centred at 45°N) and 30° in longitude (centred at 10°E).

Following Ern et al. (2004), GW momentum fluxes MF (i.e. without information on the direction) are calculated via:

$$MF = \frac{\rho}{2}\frac{k}{m}\left(\frac{g}{N}\right)^2\left(\frac{\hat{T}}{T}\right)^2, \qquad (1)$$

where ρ is the density of the background atmosphere, g is the acceleration due to gravity, N is the buoyancy frequency, k the horizontal and m the vertical wavenumber of the GW. The horizontal wavenumber has been obtained from profile pairs along the measurement track (Ern et al., 2004; 2011).

3 Results

In Figs. 3-5 prevailing winds as measured by the Collm radar are presented. JJA mean zonal prevailing winds at different altitudes are shown in Fig. 3 (left panel). The data are updated from Jacobi et al. (2011). In the lower part of the figure, F10.7 solar radio fluxes are added. One can see that, at least for lower altitudes considered, the earlier LF results are reproduced: if the years 2008 and 2009 are disregarded, a negative correlation with the solar flux is indicated, i.e. the mesospheric easterlies are stronger

during solar maximum. Keuer et al. (2007) also reported a negative solar cycle dependence of summer zonal winds. However, in Fig. 3 during the deep solar minimum this behaviour reverses. The interannual variability also confirms measurements presented by Hoffmann et al. (2011, their Fig. 3) at 80-84 km. They also found maximum winds in 2007, weaker winds in 2008/2009, and again stronger ones in 2010.

The mean winds at lower and upper heights are anticorrelated, i.e. if the mean wind is weaker (westward) at 82 km the lower thermosphere maximum is weaker (eastward), too (Figure 4, left panel). This is also seen if the mean winds are compared with the vertical shear of zonal wind (Figure 3, right panel). During years with weaker winds, especially in 2007, the wind shear values at most heights are smaller, too.

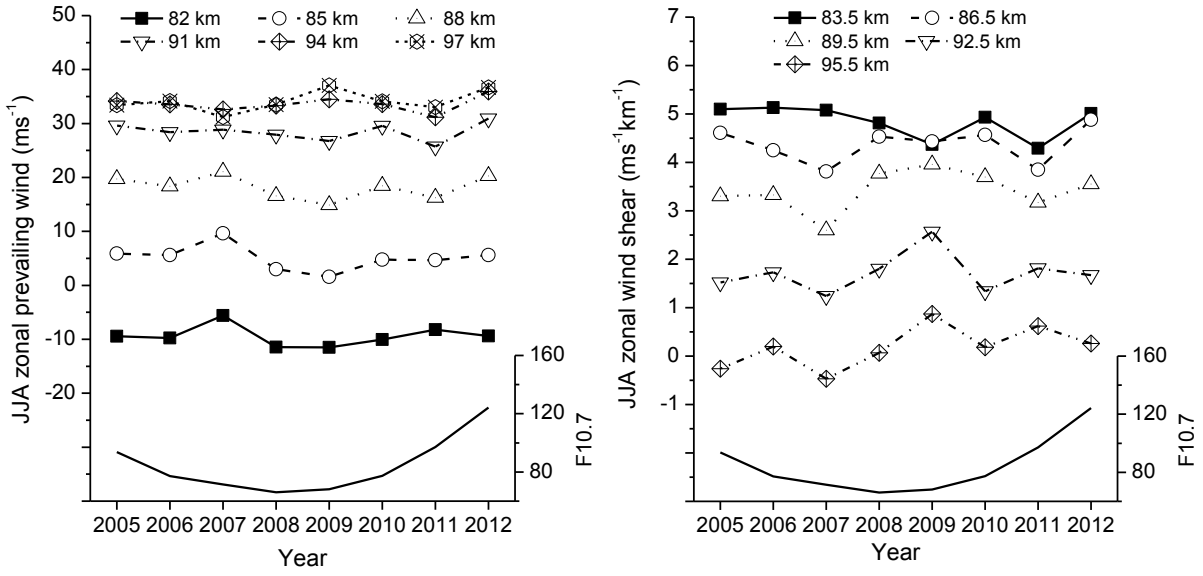

Figure 3: *Time series of June-August (JJA) mean zonal prevailing wind (left panel) and vertical shear of zonal wind (right panel) as measured by the Collm meteor radar. Seasonal mean F10.7 values are added in the lower part of the respective panels.*

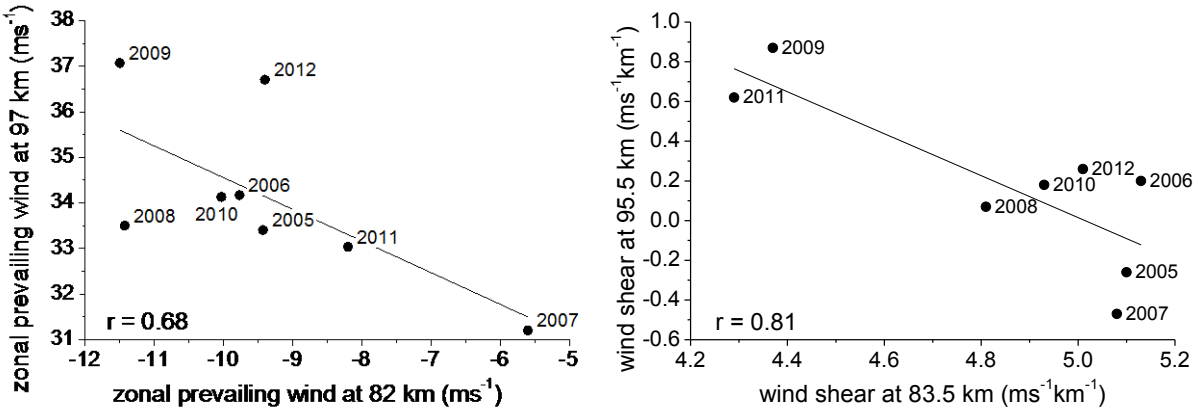

Figure 4: *June-August mean zonal prevailing wind (left panel) and vertical shear of zonal wind (right panel) at the uppermost level vs. the respective parameters at the lowermost level as measured by the Collm meteor radar 2005-2012.*

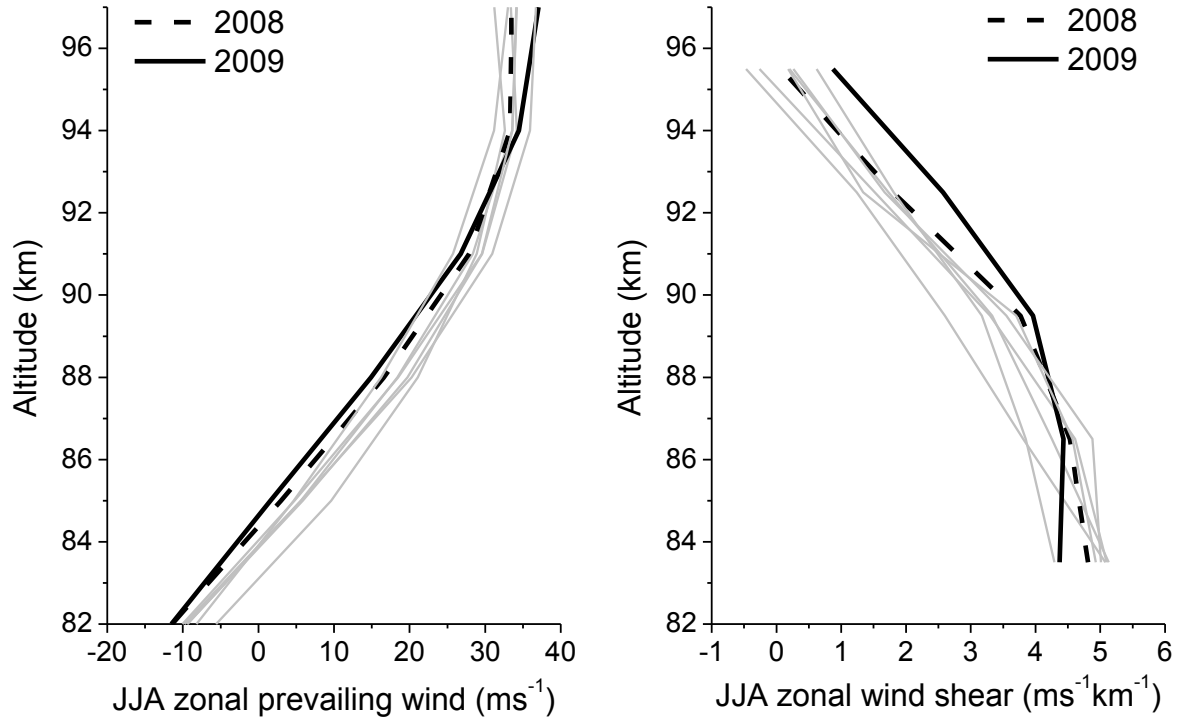

Figure 5: *Profiles of June-August mean zonal prevailing wind (left panel) and vertical shear of zonal wind (right panel) as measured by the Collm meteor radar 2005-2012. The years 2008 and 2009 are highlighted.*

However, the interannual variability of the wind shear also changes with height, so that wind shear variability at lower and higher altitudes is mainly anticorrelated (Figure 4, right panel). E.g., in 2006 the wind shear in the mesosphere (at 83.5 km) is comparatively strong. If we assume that the shear is due to GW MF divergence this would mean that at greater altitudes MF may have a tendency towards smaller values, which also implies smaller possible MF divergence there. On the contrary, in 2009 the wind shear at lower MLT heights is small, which may be explained by weaker MF divergence. Then at greater altitudes the stronger MF fluxes and MF divergence will lead to stronger wind shear then.

In Figure 5, vertical profiles of zonal mean wind and wind shear are shown. The profiles for the years 2008 and 2009, taken during the extreme solar minimum, are highlighted. They show a tendency of being shifted upward w.r.t. to the other years both in the mean wind and the wind shear profile.

The SABER squared temperature amplitudes at several heights are presented in Fig. 6. The LF variances 2002-2007 are added as solid circles/solid line to show that their interannual variability reasonably well qualitatively reproduces the temperature amplitude variability at about 90-95 km. For comparison, also JJA mean GW wind variances at 91 km as measured by the Collm radar are added (solid circles, dashed line). They also show a similar interannual variability. The SABER amplitudes at 90-100 km show a similar tendency to what has been described for the LF GW proxies already:

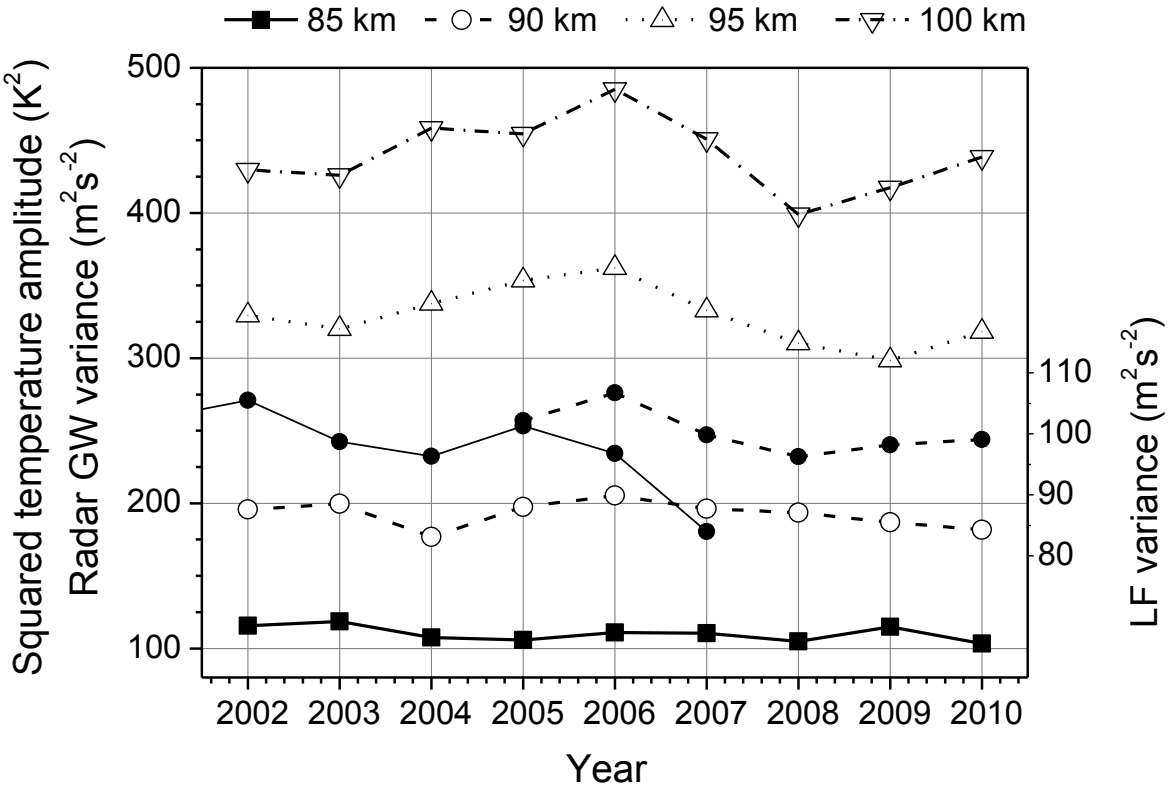

Figure 6: *SABER 10°E squared temperature amplitudes 2002-2010(solid squares, open circles, up and down open triangles) at different altitudes. LF variances at approx. 90 km from Fig. 2 (solid circles, solid lines) and GW variances from the Collm meteor radar (taken from Jacobi et al., 2011, updated from Placke et al., 2011) are added. A fixed value of 150 m^2s^{-2} has been subtracted from the meteor radar GW variances.*

after the solar maximum GW amplitudes tend to decrease, but during the descending phase of the solar cycle they increase again, before they minimise during the solar minimum.

Vertical profiles of SABER temperature amplitudes and their vertical gradients are shown in Fig. 7. Again, the years 2008 and 2009 are highlighted. It can be seen that above 90 km the amplitudes are small during solar minimum while between 80 and 85 km they are comparable with the other years, or even larger. This is reflected in the small vertical gradients above 85-95 km. These indicate stronger GW forcing of the mean flow, and connected with that stronger wind shear at these heights and stronger westerly winds in the lower thermosphere, as can be seen in Figure 3. This connection is illustrated in Fig. 8, where the vertical shear of zonal wind at about 90 km is plotted vs. the squared SABER temperature amplitude gradient at 90 km. Note, however, that in 2007 the mesospheric easterly winds were particularly weak, connected with small wind shear values. These are, however, connected with only moderately large GW amplitude increase with altitude.

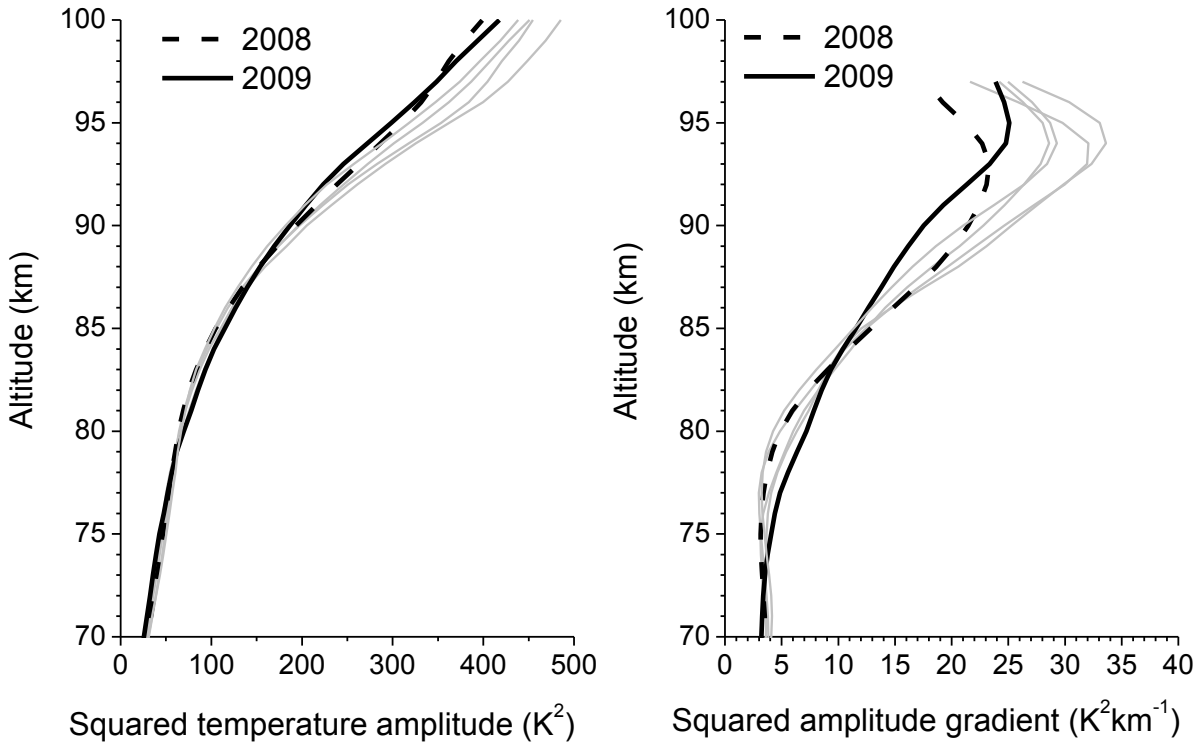

Figure 7: *SABER 10°E squared temperature amplitudes (left panel) and vertical amplitude gradient (right panel).*

Temperature amplitudes as shown in Figs 6-8 are useful because they can be compared with the LF or meteor radar wind variances in order to qualitatively validate the conclusions drawn from the latter. A more direct parameter to investigate GW-mean flow interaction, however, is the GW MF. Fig. 9 shows SABER MF time series at different altitudes. At mesospheric heights MF is broadly connected with the solar cycle, and decreases after the solar maximum, with the exception of the described increase during the descending part of the solar cycle. At greater altitudes, this behaviour partly reverses, so that there are large MF values especially in 2009. However, the interannual variability in general is more complicated and cannot easily be interpreted.

An even more suitable parameter is the MF divergence, which is shown in Fig. 10. MF divergence is usually weak in the mesosphere and thermosphere, and maximises at an altitude of 82-84 km. The peak height decreases with solar activity, so that the MF divergence, and therefore the main region where GW interact with the mean flow, is about 2 km higher during solar minimum than during solar maximum. This results in an anticorrelation of MF divergence taken slightly below and above the peak (Figure 11). The upward shift of the MF divergence profile during solar minimum may explain the upward shift of wind and wind shear profiles shown in Fig.5.

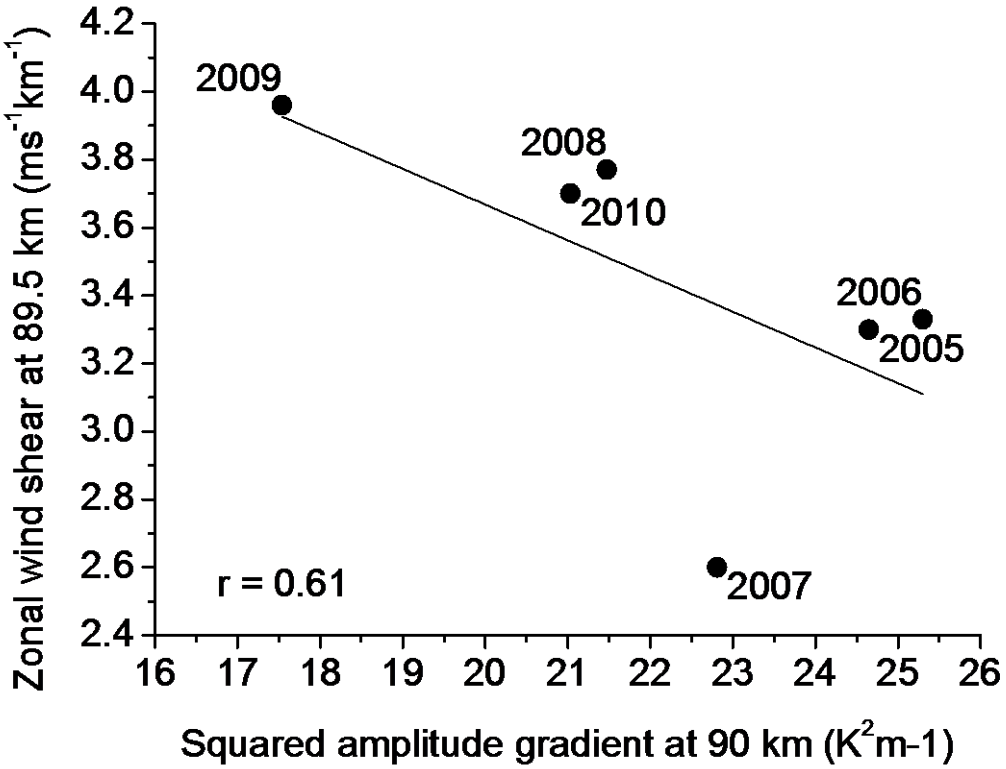

***Figure 8**: SABER squared temperature amplitude gradient at 90 km vs. vertical shear of zonal wind.*

4 Discussion

As can be seen from Figs 2 and 6, GW amplitudes are modulated with the solar cycle so that large amplitudes are found during solar maximum. This behaviour changes and partly reverses during the descending phase of the solar cycle. The corresponding MF time series in Figure 9 clearly show this for the upper mesosphere. Concerning GW mean flow interaction, there is, at least during the time interval 2002-2010, a possible solar cycle modulation of the height of the peak MF divergence (Fig. 10). During solar maximum, when mesospheric MF are largest, they tend to decrease at lower altitudes (MF divergence peak already at 82 km) than during solar minimum (at about 84 km).

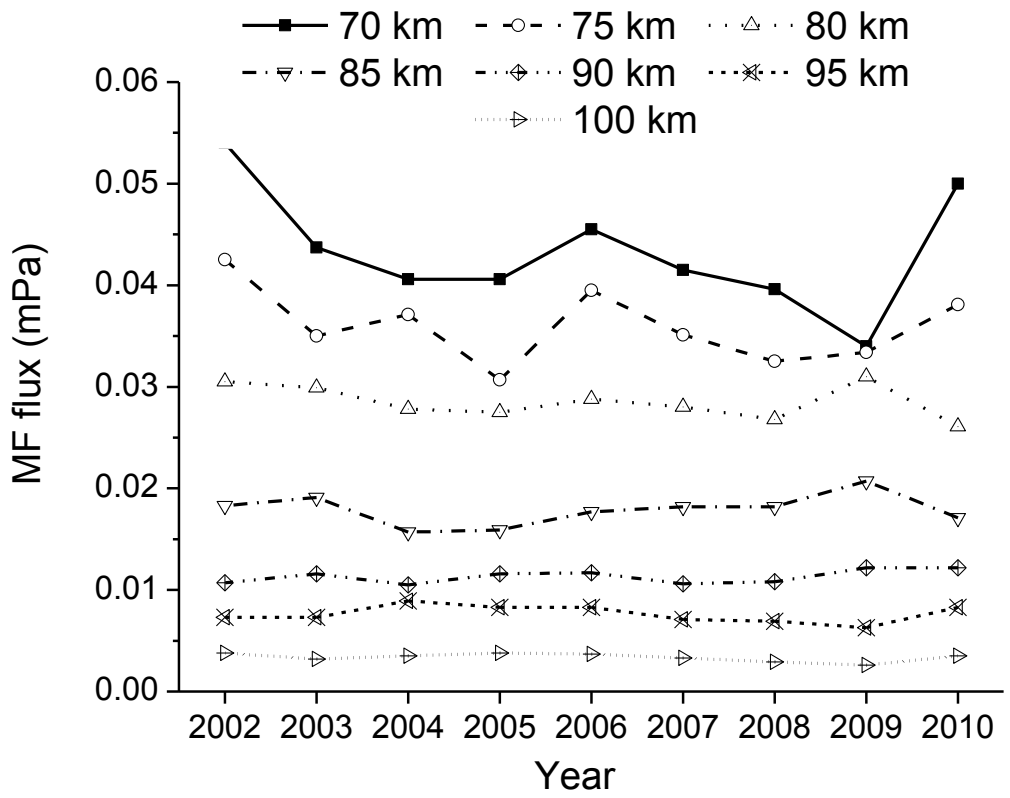

Figure 9: *Time series of SABER MF at 10°E and at different altitudes.*

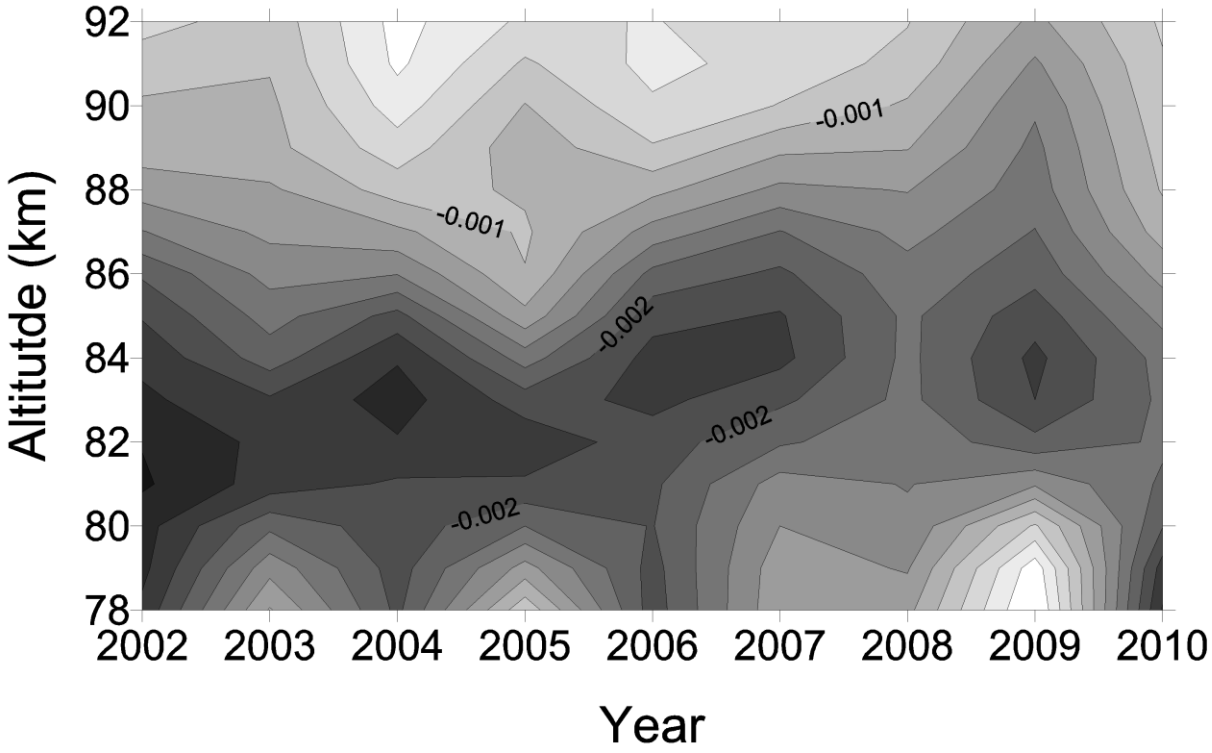

Figure 10: *SABER MF divergence at 10°E.*

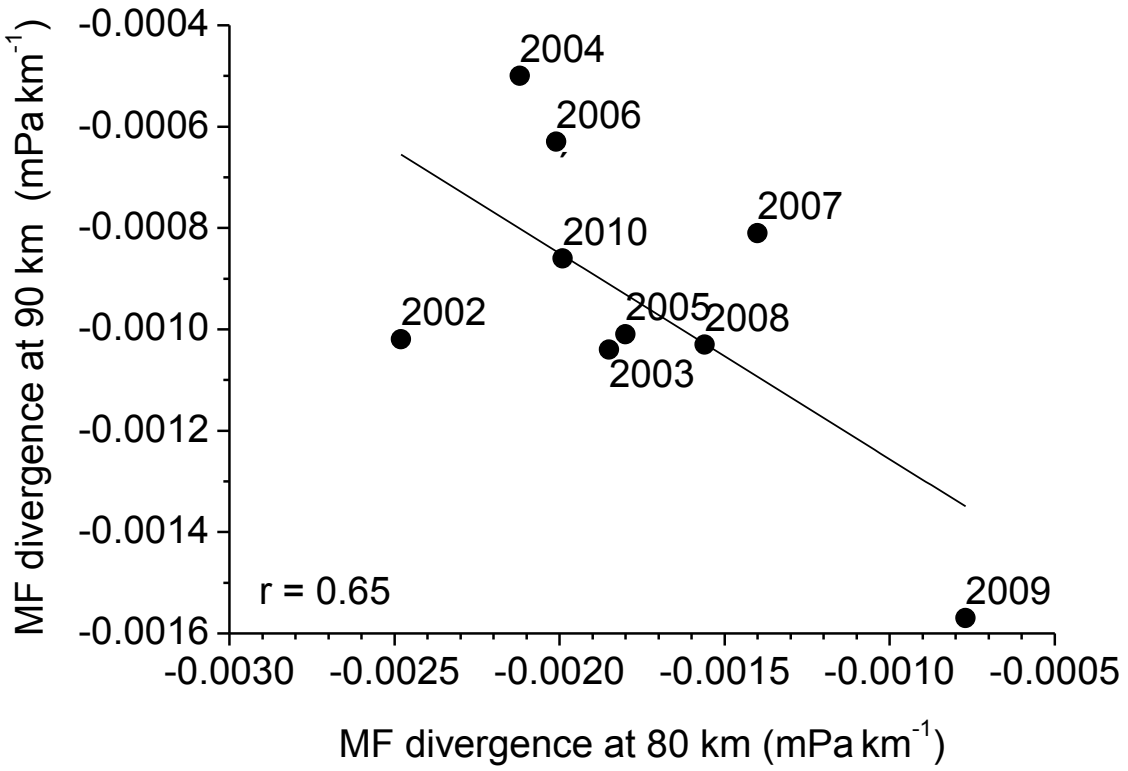

Figure 11: *SABER MF divergence at 10°E at 90 km altitude vs. the respective values at 80 km.*

A possible general picture thus is that the mesospheric zonal wind jet tends to be stronger during solar maximum (e.g., Schmidt at al., 2006). This may, assuming that GW are saturated and therefore the amplitudes are proportional to the intrinsic phase speed, lead to larger GW amplitudes then. However, GW seem to break earlier (at lower altitudes, as seen in Fig. 10) during solar maximum than during solar minimum. Therefore, the measured GW amplitude variability observed in the MLT probably results from a mixture of at least two processes. The first one is due to the larger/smaller GW amplitudes in the mesosphere during solar maximum/minimum. The second is the weaker MF divergence in the mesosphere during solar minimum, which in the MLT may counteract the first effect. A superposition of both may explain that MLT GW amplitudes are strong during solar maximum (due to the first effect) and during years of moderately low solar flux, when the second effect may be more effective, before during solar minimum the first effect again may take over.

The interannual variation of the MF divergence may explain part of the observed behaviour of winds. Comparing Figs. 3 and 10 we see that (except for the year 2007) there is a tendency for a decrease of both MF divergence and vertical shear of zonal wind at 83.5 km (the lowermost level where we have radar wind shear) until 2009, and then again an increase. At greater altitudes, we have the opposite behaviour in both parameters.

The year 2007 is, regarding the radar winds in Figs. 3-5, different from other ones. In the upper mesosphere the zonal wind values were weak. This was connected with a weak mesospheric jet, which also has been found by Hoffmann et al. (2011, their Fig. 3). However, this behaviour different from other years is not reflected in a similarly strong change of GW amplitudes or MF, and the reason is unclear. Obviously, there are other possible sources of MLT wind and GW variability than a pure solar cycle modulation, e.g. changes of GW sources and other variations of the mesospheric circulation.

5 Conclusions

We have analysed summer zonal mean MLT winds over Collm together with GW analyses from SABER from 2002-2010 to get more insight into the sources of interannual wind variability. MLT GW MF are stronger during solar maximum than during solar minimum, and there is a secondary maximum during the descending phase of the solar cycle. This confirms earlier results from LF measurements, and a comparison of LF wind variances with SABER squared temperature amplitudes show very good qualitative agreement.

The variability of GW in the course of a solar cycle may be partly explained by a superposition of a solar cycle in the mesospheric wind jet that leads to larger GW amplitudes during solar maximum, and an upward shift of the region of maximum GW-mean flow interaction during solar minimum. This upward shift may be explained by the fact that small-amplitude GW generally tend to break at lower altitudes than large-amplitude GW. This upward shift may also explain the upward shift of the observed wind and wind shear profiles during solar minimum, leading to a reversal of the (otherwise negative) solar cycle effect in zonal winds then.

The effects outlined here are clearly not the only sources of variability in MLT GW and winds. Examples are the large MF values in 2006, probably due to a strong mesospheric jet, or the very weak winds, both mesospheric eastward and lower thermospheric westward, in 2007. In a further study we shall analyse mesospheric winds derived from SABER temperatures as well.

The results presented here are based on local radar data and satellite data from a 30°×10° longitude/latitude window. An interesting question is also, whether the solar cycle effect is as well visible in zonal mean data, or whether the effects are of local nature. Radar MLT mean winds taken at different longitudes (Canada, Central Europe, and Eastern Europe) partly showed strong differences at the decadal time scale (Jacobi et al., 2012). This should also be addressed in a future study.

Acknowledgements

SABER data were provided by GATS Inc. Many thanks also go to the teams of the SABER instruments for all their effort to create the excellent data sets. F10.7 solar radio flux data have been provided by NGDC through ftp access on ftp://ftp.ngdc.noaa.gov/STP/SOLAR_DATA/.

References

Ern, M., Preusse, P., Alexander, M.J., Warner, C.D., 2004: Absolute values of gravity wave momentum flux derived from satellite data. J. Geophys. Res., 109, D20103, doi:10.1029/2004JD004752.

Ern, M., Preusse, P., Gille, J.C., Hepplewhite, C.L., Mlynczak, M.G., Russell III, J.M., Riese, M., 2011: Implications for atmospheric dynamics derived from global observations of gravity wave momentum flux in stratosphere and mesosphere. J. Geophys. Res. 116, D19107, doi:10.1029/2011JD015821.

Hocking, W.K., 2005: A new approach to momentum flux determinations using SKiYMET meteor radars. Ann. Geophys. 23, 2433–2439.

Hoffmann, P., Rapp, M., Singer, W., Keuer, D., 2011: Trends of mesospheric gravity waves at northern middle latitudes during summer. J. Geophys. Res. 116, D00P08, doi:10.1029/2011JD015717.

Jacobi, Ch., 2011: Meteor radar measurements of mean winds and tides over Collm (51.3°N, 13°E) and comparison with LF drift measurements 2005-2007. Adv. Radio Sci. 9, 335-341.

Jacobi, Ch., Schminder, R., Kürschner, D., 1996: On the influence of the stratospheric quasi-biennial oscillation on the mesopause zonal wind over Central Europe. Meteorol. Zeitschrift, N.F. 5, 318-323.

Jacobi, Ch., Gavrilov, N.M., Kürschner, D., Fröhlich, K., 2006: Gravity wave climatology and trends in the mesosphere/lower thermosphere region deduced from low-frequency drift measurements 1984-2003 (52.1°N, 13.2°E). J. Atmos. Solar-Terr. Phys. 68, 1913-1923.

Jacobi, Ch., Hoffmann, P., Placke, M., Stober, G., 2011: Some anomalies of mesosphere/lower thermosphere parameters during the recent solar minimum. Adv. Radio Sci. 9, 343-348.

Jacobi, Ch., Hoffmann, P., Liu, R.Q., Merzlyakov, E.G., Portnyagin, Yu.I., Manson, A.H., Meek, C.E., 2012: Long-term trends, their changes, and interannual variability of Northern Hemisphere midlatitude MLT winds. J. Atmos. Solar-Terr. Phys., 75-76, 81-91, doi:10.1016/j.jastp.2011.03.016.

Keuer, D., Hoffmann, P., Singer, W., Bremer, J., 2007: Long-term variations of the mesospheric wind field at mid-latitudes. Ann. Geophys., 25, 1779–1790.

Muller H.G., Nelson L., 1978: A travelling quasi 2-day wave in the meteor region. J. Atmos. Terr. Phys., 40, 761- 766.

Placke, M., Stober, G., Jacobi, Ch., 2011: Gravity wave momentum fluxes in the MLT—Part I: Seasonal variation at Collm (51.3°N, 13.0°E). J. Atmos. Solar–Terr. Phys., 73, 904-910, doi:10.1016/j.jastp.2010.07.012.

Schmidt, H., Brasseur, G.P., Charron, M. , Manzini, E., Giorgetta, M.A., Diehl, T., Fomichev, V.I., Kinnison, D., Marsh, D., Walters, S., 2006: The HAMMONIA chemistry climate model: Sensitivity of the mesopause region to the 11-year solar cycle and CO2 doubling. J. Climate, 19, 3903-3931.

Addresses of Authors

Christoph Jacobi, Institut für Meteorologie, Universtiät Leipzig, Stephanstr. 3, 04103 Leipzig.

Manfred Ern: Forschungszentrum Jülich GmbH, Institut für Energie- und Klimaforschung, IEK-7: Stratosphäre, 52425 Jülich.